ResearchGate

See discussions, stats, and author profiles for this publication at: https://www.researchgate.net/publication/228974469

A General Framework for the Analysis of Metamaterial Transmission Lines

Article *in* Progress In Electromagnetics Research B · January 2010

DOI: 10.2528/PIERB10030601

CITATIONS
4

READS
97

1 author:

Giulio Antonini
Università degli Studi dell'Aquila
347 PUBLICATIONS **3,410** CITATIONS

SEE PROFILE

Some of the authors of this publication are also working on these related projects:

PEEC-Book View project

DWS/PWLFIT View project

All content following this page was uploaded by Giulio Antonini on 04 June 2014.

The user has requested enhancement of the downloaded file.

Progress In Electromagnetics Research B, Vol. 20, 353–373, 2010

A GENERAL FRAMEWORK FOR THE ANALYSIS OF METAMATERIAL TRANSMISSION LINES

G. Antonini

UAq EMC Laboratory
Dipartimento di Ingegneria Elettrica e dell'Informazione
Universit degli Studi dell'Aquila
Via G. Gronchi 18, 67100, L'Aquila, Italy

Abstract—This paper presents a closed-form analysis of composite right/left handed transmission lines. The ladder network structure of the transmission line allows to obtain a rational form of any two-port network representation. As a consequence of the rational form of the transfer functions, poles and residues are easily computed and the dominant ones selected leading to an efficient time-domain macromodel. The numerical results confirm the robustness and the accuracy of the proposed method in capturing the physics of composite right/left handed transmission lines.

1. INTRODUCTION

The idea of materials with both negative real permittivity ε and permeability μ was initially theoretically introduced by Veselago in 1968 [1, 2]. These materials are referred to as double-negative or left-handed materials. Such a topic has recently received a renewed interest as a consequence that experimental evidence of left-handed (LH) materials properties has been given by Smith et al. [3, 4] who demonstrated an LH structure made of negative-ε thin-wires and negative-μ split-ring resonators exhibiting anomalous refraction at the boundary. Since then many different applications of metamaterials have been developed [5–7]. Among the others, artificial transmission lines have been presented which can mimic the propagation characteristics of TEM-based transmission systems filled with homogeneous, linear and isotropic negative refraction index bulk media.

Initially, a transmission line approach of left-handed (LH) materials has been presented [8] where an equivalent circuit for a

Corresponding author: G. Antonini (giulio.antonini@univaq.it).

left-handed transmission line (LH-TL) is proposed. Such equivalent circuit has been then extended to composite right/left handed (CRLH) metamaterials [9]. A more complex unit cell of the equivalent line circuit of a metamaterial constituted by a split-ring resonator/wire medium is presented [10]. Two-dimensional (2-D) composite right/left handed transmission lines (CRLH-TLs) have been presented [11, 12].

More recently, new metamaterial transmission lines have been proposed which exhibit a more complex frequency behavior [13–17].

In all these works, the properties of CRLH-TLs are derived from the corresponding ideal homogeneous transmission line or using the image-parameter filter theory according to which, the properties of the periodic structure can be obtained from the properties of its unit-cell [18, 19]. In the latest years, there has also been an increasing interest for characterizing CRLH-TLs in time-domain [20, 21]. In particular, In [20], the method of moments is used to integrate the Telegrapher's equations. In [21], the impulse-regime propagation along CRLH-TLs is examined using the inverse Fourier transform of frequency-domain results obtained by means of a matched transmission line model.

This work presents a systematic modeling of CRLH-TLs which is based on the analytical characterization of the half-T ladder network (HTLN) constituting the CRLH-TL. Due to the discrete nature of the structure, in the following, we will refer to composite right/left handed ladder networks (CRLH-LNs) to distinguish them from the homogeneous composite right/left handed transmission lines (CRLH-TLs). The proposed approach provides a rational form of two-port parameters of the CRLH-TL, leading to machine-accuracy computation of its poles; furthermore, the knowledge of the CRLH-LN poles allows to generate a rigorous macromodel which can be used in both time and frequency-domain, in conjunction with linear and non-linear terminations. It is worth noticing that the proposed method can be used for any topology of the unit-cell, which can be eventually dispersive, since no assumption is done on it, besides assuming that it is modeled in terms of lumped elements. It is also to be observed that the resulting time-domain macromodel can be used to investigate novel complex dispersive transient phenomena [21].

Comparisons are made with results obtained by using the inverse Fourier transform of frequency-domain-based results, according to the guidelines of IEEE Standard P1597 [22] and in particular by means of the feature selective validation (FSV) technique [23, 24].

The paper is organized as follows. The rational two port representation of the CRLH-LN is presented in Section 2. The dispersion relation of CRLH-LNs is obtained and the limitations

in using the homogeneous transmission line model are pointed out in Section 3. The time-domain model is presented in Section 4: the derivation of the poles/residues model is described in Section 4.1 and the synthesis of the time-domain macromodel are described in Section 4.2. Numerical results for CRLH-LNs are presented in Section 5, validating the proposed technique. Finally, the conclusions are drawn in Section 6.

2. POLYNOMIAL MODEL OF CRLH-LNS

Composite right/left handed transmission lines can be modeled as the cascade of n elementary identical cells, as shown in Figure 1, along with input and output port voltages and currents.

Let us assume to know the $ABCD$ matrix of the elementary cell $C_k, k = 1, \ldots, n$ from measurement or simulations. A possible equivalent circuit synthesizing the elementary cell is shown in Figure 2 where the π circuit is used; alternative models such as the T circuit are obviously acceptable as well. The elementary cell is characterized by series impedance $Z_l(s)$ and shunt admittances $Y_{t1}(s)$ and $Y_{t2}(s)$ which can be directly obtained from the $ABCD$ matrix or the S-parameters of the elementary cell [25].

A half-T ladder network (HTLN) can be identified within the 1-D periodic structure generated by cascading n elementary cells, as shown in Figure 3 for $n = 3$.

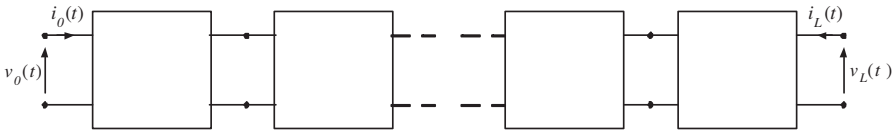

Figure 1. Composite right/left handed transmission transmission line.

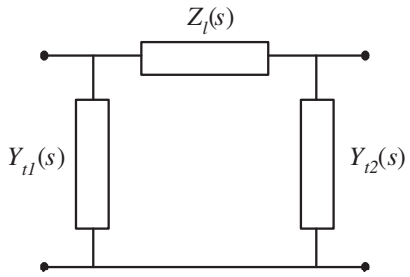

Figure 2. Elementary cell of the periodic structure.

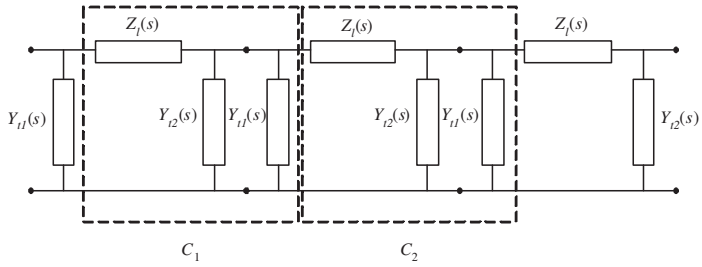

Figure 3. Half-T ladder network within the CRLH periodic structure.

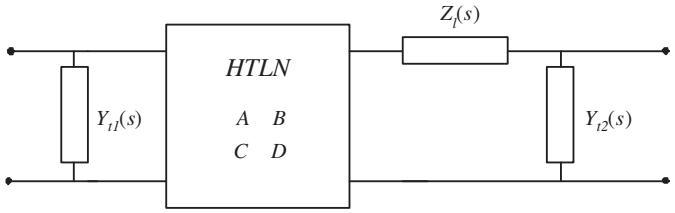

Figure 4. Equivalent model of the CRLH periodic structure.

The knowledge of the the impedance $Z_l\,(s)$ and admittances $Y_{t1}\,(s)$ and $Y_{t2}\,(s)$, which may represent both lumped or distributed elements, allows the series impedance $Z_1(s)$ and shunt admittance $Y_2(s)$ of the half-T ladder network to be written in the Laplace domain as

$$Z_1\,(s) \;=\; Z_l\,(s) \tag{1a}$$

$$Y_2\,(s) \;=\; Y_{t1}\,(s) + Y_{t2}\,(s) \tag{1b}$$

The residual admittances and impedances on the left and right ends of the circuit (see Figure 3) can be incorporated as simple two-port networks [26]. Hence, the overall structure can be regarded as the cascade of three sub-systems, the left-end shunt admittance $Y_{t1}\,(s)$, the HTLN structure, the right-end two port network comprising $Z_l\,(s)$ and $Y_{t2}\,(s)$, as shown in Figure 4. The $ABCD$-parameters of the left and right-end circuits can be easily obtained from $Z_l\,(s)\,, Y_{t1}\,(s)$ and $Y_{t2}\,(s)$ [26].

Once the time-domain macromodel of the HTLN is obtained, left- and right-end circuits can be easily taken into account by using modified nodal analysis (MNA) stamps [27, 28]. For this reason, in the following, we will refer to CRLH-LNs. In the more general case of arbitrary complex unit cells, a rational model can be associated to

$Z_1(s)$ and $Y_2(s)$ which reads:

$$Z_1(s) = \frac{N_{Z_1}(s)}{D_{Z_1}(s)} \tag{2a}$$

$$Y_2(s) = \frac{N_{Y_2}(s)}{D_{Y_2}(s)} \tag{2b}$$

In the following, for the sake of simplicity, the topology shown in Figure 5 is adopted for the unit cell of the CRLH-LN, which is characterized by both series and shunt inductances and capacitances [9]. In addition, series resistances and shunt conductances are added to take the ever existing losses into account. The equivalent circuit shown in Figure 5 represents a possible model of the unit cell although several more general topologies can be considered [8, 18].

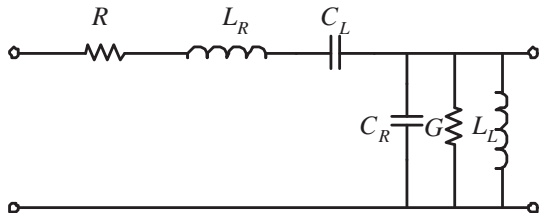

Figure 5. Elementary half-T cell for a composite right/left handed ladder network (CRLH-LN).

To the aim of developing the closed-form macromodel of a CRLH-LN, it is useful to define the unit cell impedance and admittance in the Laplace domain:

$$Z_1(s) = R + sL_R + \frac{1}{sC_L} = \frac{s^2 L_R C_L + sRC_L + 1}{sC_L} \tag{3a}$$

$$Y_2(s) = G + sC_R + \frac{1}{sL_L} = \frac{s^2 L_L C_R + sGL_L + 1}{sL_L} \tag{3b}$$

which are rational functions.

In Ref. [29], it has been shown that a half-T ladder network can be analytically characterized in terms of closed-form polynomials which can be related to Chebyschev polynomials [30]. In the following it will be briefly summarized the polynomial based approach. To this aim, let us define the half-T cell factor $K(s)$ as:

$$K(s) = Z_1(s)\, Y_2(s) \tag{4}$$

In Ref. [29], it was shown that all the electrical characteristics of a HTLN can be expressed in terms of two polynomials (namely DFF

and DFFz) depending on the cell matrix factor $K(s)$:

$$P_b^n(K(s)) = \sum_{j=0}^{n} b_{j,n} K^j(s) \qquad \text{DFF polynomial of order } n \quad (5)$$

$$P_c^n(K(s)) = \sum_{j=0}^{n} c_{j,n} K^{j+1}(s) \qquad \text{DFFz polynomial of order } n \quad (6)$$

where $K^j(s)$ is the j-th power of $K(s)$ and coefficients $b_{j,n}$ and $c_{j,n}$ can be computed analytically as in Ref. [29], reported here for the sake of clarity:

$$b_{i,j} = \begin{pmatrix} i+j \\ j-i \end{pmatrix} \quad (7a)$$

$$c_{i,j} = \begin{pmatrix} i+j+1 \\ j-i \end{pmatrix} \quad (7b)$$

Polynomial coefficients b and c can be cast in triangles known as DFF and DFFz triangles [29], shown in Table 2. It is worth pointing out that the polynomial coefficients reduce to Fibonacci's numbers when $Z_1(s) = Y_2(s)^{-1}$ so that $K(s) = 1$ [29].

Table 1. DFF triangle.

i^j	0	1	2	3	4
0	1				
1	1	1			
2	1	3	1		
3	1	6	5	1	
4	1	10	15	7	1
...	.....				

Table 2. DFFz triangle.

i^j	0	1	2	3	4
0	1				
1	1	1			
2	1	3	1		
3	1	6	5	1	
4	1	10	15	7	1
...	.....				

Two port A, B, C and D parameters can be expressed in terms of DFF and DFFz polynomials as:

$$A(s) = \sum_{j=0}^{n} b_{j,n} K^j(s) = P_b^n(K(s)) \tag{8a}$$

$$B(s) = \left(\sum_{j=0}^{n} c_{j,n} K^{j+1}(s) \right) \cdot Y_2^{-1}(s) = P_c^n(K(s)) \cdot Y_2^{-1}(s) \tag{8b}$$

$$\begin{aligned} C(s) &= Z_1^{-1}(s) \cdot \left(\sum_{j=0}^{n} c_{j,n} K^{j+1}(s) \right) \\ &= Z_1^{-1}(s) \cdot P_c^n(K(s)) \end{aligned} \tag{8c}$$

$$D(s) = \sum_{j=0}^{n-1} b_{j,n-1} K^j(s) = P_b^{n-1}(K(s)) \tag{8d}$$

The knowledge of the $ABCD$ parameters in a polynomial form allows to obtain any other two port matrix representation in a rational form. It is to be remarked that the proposed polynomial formulation provides an exact characterization of the half-T ladder network and is totally independent on the topology of impedance $Z_l(s)$ and admittances $Y_{t1}(s), Y_{t2}(s)$ which can be represented by any lumped or distributed linear network. It is also worth noticing that the $ABCD$-parameters of the half-T ladder network are computed in a polynomial form, thus completely avoiding any matrix product.

The Y parameters can be evaluated as:

$$Y_{11}(s) = DB^{-1} = P_b^{n-1}(K(s)) \cdot \left(P_c^n(K(s)) \cdot Y_2^{-1}(s) \right)^{-1} \tag{9a}$$

$$Y_{12}(s) = -B^{-1} = -\left(P_c^n(K(s)) \cdot Y_2^{-1}(s) \right)^{-1} \tag{9b}$$

$$Y_{21}(s) = -B^{-1} = -\left(P_c^n(K(s)) \cdot Y_2^{-1}(s) \right)^{-1} \tag{9c}$$

$$Y_{22}(s) = AB^{-1} = P_b^n(K(s)) \cdot \left(P_c^n(K(s)) \cdot Y_2^{-1}(s) \right)^{-1} \tag{9d}$$

It is to be observed that $Y_{22}(s)$ is an improper function and it can be expressed in terms of $Y_{11}(s)$ as:

$$Y_{22}(s) = Y_{11}(s) + Y_2(s) \tag{10}$$

Polynomials $P_b^{n-1}(K(s))$ and $P_c^n(K(s))$ can be factored into zero-pole pairs. Their factorization is accomplished by using the poles given by the expressions presented in Ref. [30]:

$$P_b^{n-1}(K(s)) = \prod_{j=1}^{n-1} (K(s) - u_{j,n-1}) \tag{11a}$$

$$P_c^n\left(K(s)\right) = \prod_{j=1}^{n-1}\left(K(s) - v_{j,n-1}\right)\cdot K \tag{11b}$$

The previous expressions (9a) and (9c), taking into account that $K(s)\cdot Y_2^{-1}(s) = Z_1(s)$, can be factored in the following way:

$$Y_{11}(s) = \prod_{j=1}^{n-1}\left(K(s) - u_{j,n-1}\right)\cdot \Psi(s)^{-1} \tag{12a}$$

$$Y_{21}(s) = Y_{12}(s) = -\Psi(s)^{-1} \tag{12b}$$

$$Y_{22}(s) = \prod_{j=1}^{n}\left(K(s) - u_{j,n}\right)\cdot \Psi(s)^{-1} \tag{12c}$$

where

$$\Psi(s) = \left[\prod_{j=1}^{n-1}\left(K(s) - v_{j,n-1}\right)\cdot Z_1(s)\right] \tag{13}$$

Roots $u_{j,n-1}$ and $v_{j,n-1}$ are given by the following expressions [31]:

$$u_{j,n} = -4\sin^2\left[\frac{(2j-1)}{(2n+1)}\frac{\pi}{2}\right] \tag{14a}$$

$$v_{j,n} = -4\sin^2\left[\frac{j}{(n+1)}\frac{\pi}{2}\right] \tag{14b}$$

Similar rational expressions can be obtained for the Z parameters, the hybrid H/G parameters, the S parameters. For instance, the Z parameters read:

$$Z_{11}(s) = AC^{-1} = P_b^{n-1}\left(K(s)\right)\cdot\left(P_c^n\left(K(s)\right)\cdot Z_1^{-1}(s)\right)^{-1} \tag{15a}$$

$$Z_{12}(s) = -C^{-1} = -\left(P_c^n\left(K(s)\right)\cdot Z_1^{-1}(s)\right)^{-1} \tag{15b}$$

$$Z_{21}(s) = -C^{-1} = -\left(P_c^n\left(K(s)\right)\cdot Z_1^{-1}(s)\right)^{-1} \tag{15c}$$

$$Z_{22}(s) = DC^{-1} = P_b^n\left(K(s)\right)\cdot\left(P_c^n\left(K(s)\right)\cdot Z_1^{-1}(s)\right)^{-1} \tag{15d}$$

Once the port voltage is obtained, the voltage at the generic node β in the Laplace-domain can be expressed as [29]:

$$V_\beta(s) = \frac{P_b^{n-\beta}\left(K(s)\right)}{P_b^n\left(K(s)\right)}V_0(s) \tag{16}$$

The general expression of the series branch current $I_{\beta 1}(s)$ is:

$$I_{\beta 1}(s) = \frac{1}{Z_1(s)}\frac{P_c^{n-\beta+1}\left(K(s)\right)}{P_b^n\left(K(s)\right)}V_0(s) \tag{17}$$

Similarly, the shunt branch current $I_{\beta 2}(s)$ can be expressed as:

$$I_{\beta 2}(s) = \frac{1}{Z_2(s)} \frac{P_b^{n-\beta}(K(s))}{P_b^n(K(s))} V_0(s) \tag{18}$$

It is to be noticed that the proposed technique allows to compute each matrix entry of any two-port representation of the CRLH-LN separately from the others. For the $ABCD$ two-port representation, this avoids the cumbersome matrix product, providing directly the final matrix, thus providing a significant cpu-time saving when the parameters are computed over a wide frequency range. It is also worth to be observed that the frequency dependence of the unit cell parameters is completely described by the cell factor $K(s)$ and that the roots $u_{j,n-1}$ and $v_{j,n-1}$ of $P_b^{n-1}(K(s))$ and $P_c^n(K(s))$ polynomials are frequency independent [29].

3. DISPERSION RELATION OF CRLH-LNS

To determine the dispersion relation of a CRLH-LN the Bloch-Floquet theorem is applied. To this aim, periodic boundary conditions are enforced to the unit cell represented by its $ABCD$ matrix, leading to an eigenvalue problem which reads:

$$\begin{bmatrix} A & B \\ C & D \end{bmatrix} \cdot \begin{bmatrix} V_{in} \\ I_{in} \end{bmatrix} = \psi \begin{bmatrix} V_{in} \\ I_{in} \end{bmatrix} \tag{19}$$

where the eigenvalues are $\psi_n = e^{-\gamma_n \ell}$. The $ABCD$ parameters of a half-T unit cell are:

$$A = 1 + Z_1 Y_2 \tag{20a}$$
$$B = Z_1 \tag{20b}$$
$$C = Y_2 \tag{20c}$$
$$D = 1 \tag{20d}$$

The computation of the eigenvalues ψ_n allows to identify the propagation, attenuation and phase constants obtained as:

$$\gamma_n = -\frac{1}{\ell} \log \psi_n \tag{21a}$$
$$\alpha_n = \mathrm{Re}(\gamma_n) \tag{21b}$$
$$\beta_n = \mathrm{Im}(\gamma_n) \tag{21c}$$

For a half-T unit cell, the propagation constant is

$$\gamma = -\frac{1}{\ell} \log \left(1 + \frac{Z_1 Y_2}{2} \pm \sqrt{\left(1 + \frac{Z_1 Y_2}{2} \right)^2 - 1} \right) \tag{22}$$

where ℓ is the length of the unit cell.

If the electrical length of the unit cell is small, some approximation can be assumed (see [9]) and the propagation constant reduces to that of a homogeneous transmission line [6]. Nevertheless, such condition fails to be applied at low frequencies where the impact of C_L and L_L is more significant. This fact causes the phase constant to significantly differ at low frequencies from that of the homogeneous transmission line. Furthermore, the same phenomenon appears at higher frequencies, at the edge of the Brillouin zone [6] Hence, the transmission line model cannot be used for accurate broadband time-domain analysis of CRLH-LN structures.

4. TIME-DOMAIN MODELS

The development of a time-domain macromodel requires as preliminary step to identify poles and residues of the rational transfer functions modeling the CRLH-LN.

4.1. Computation of Poles and Residues

Poles of Y matrix functions are obtained as the zeros of the following equation:

$$\left[\prod_{j=1}^{n-1}\left(K\left(s\right)-v_{j,n-1}\right)\cdot Z_1\left(s\right)\right]=0 \tag{23}$$

which requires n equations to be solved separately.

The poles of the CRLH-LN can be identified as:

(i) the zeros of polynomial $Z_1\left(s\right)$

(ii) the zeros of polynomial $K\left(s\right)-v_{j,n-1}$, for $j=1,\ldots,n-1$

Poles of the first type (i) satisfy the equation:

$$N_{Z_1}(s)=0 \tag{24}$$

Poles of the second type (ii) are obtained as the solutions of the equation

$$K\left(s\right)-v_{j,n-1}=0,\quad \text{for } j=1,\ldots,n-1 \tag{25}$$

which can be re-written as

$$N_{Z_1}(s)N_{Y_2}(s)-v_{j,n-1}D_{Z_1}(s)D_{Y_2}(s)=0,\quad \text{for } j=1,\ldots,n-1 \tag{26}$$

It is to be pointed out that the poles of the CRLH-LN can be computed by solving low order algebraic equations. The explicit knowledge of the poles allows to select the dominant ones. A suitable pole-pruning

strategies is described in Ref. [32]. Examples of computation of poles by using the proposed polynomial representation can be found in Ref. [32] where it is shown that a very good accuracy is achieved in finding poles of multiconductor transmission lines.

More complex topologies of the unit cell can also be considered. The only difference relies on the order of the algebraic equation (26) which, if larger than 4, cannot be solved analytically and requires a numerical solution to provide the poles. The computation of residues of pole p_i can be accomplished by using standard techniques [28]:

$$R_{11,i} = R_{22,i} = \mathrm{adj}\left[\left(\prod_{j=1}^{n-1}\left(K(s) - v_{j,n-1}\right)\right)\cdot Z_1(s)\right] / \det\left[\left(\prod_{j=1}^{n-1}\left(K(s) - v_{j,n-1}\right)\right)\cdot Z_1(s)\right] \cdot \prod_{j=1}^{n-1}\left(K(s) - u_{j,n-1}\right)(s - p_i)|_{s=p_i} \tag{27a}$$

$$R_{12,i} = R_{21,i} = -\mathrm{adj}\left[\left(\prod_{j=1}^{n-1}\left(K(s) - v_{j,n-1}\right)\right)\cdot Z_1(s)\right] / \det\left[\left(\prod_{j=1}^{n-1}\left(K(s) - v_{j,n-1}\right)\right)\cdot Z_1(s)\right]\cdot(s - p_i)|_{s=p_i} \tag{27b}$$

for $i = 1, \ldots, P_Y$, being adj$(\cdot)$ the adjoint operator of the matrix in argument and P_Y the total number of poles of the $\vec{Y}$ matrix entries.

4.2. Time-domain Macromodel Realization

Once the poles-residues representation of the Y parameters is obtained, a macromodel can be easily derived by generating the $\mathcal{E}\mathcal{A}\mathcal{B}\mathcal{C}\mathcal{D}$ state-space domain representation leading to a set of first order differential equations which reads:

$$\mathcal{E}\frac{d}{dt}x(t) = \mathcal{A}x(t) + \mathcal{B}v(t) \tag{28a}$$

$$i(t) = \mathcal{C}x(t) + \mathcal{D}v(t) \tag{28b}$$

where $\mathcal{E} \in R^{p\times p}$, $\mathcal{A} \in R^{p\times p}$, $\mathcal{B} \in R^{p\times n}$, $\mathcal{C} \in R^{n\times p}$, $\mathcal{D} \in R^{n\times n}$, p is the number of states and n the order of the proposed model. Vectors

$v(t) = [v_0(t), v_L(t)]^T$ and $i(t) = [i_0(t), i_L(t)]^T$ contain the port voltages and currents at time t, respectively.

The standard minimal-order realization techniques can be efficiently used [33–36] to generate a state-space model of the CRLH-LN. The set of first order differential Equation (28) is then augmented with the terminal conditions which, assuming linear and non-linear terminations of resistive and capacitive type, read

$$\begin{aligned} i_0(t) &= v_{s0}(t) - G_{l,0}v_0(t) - C_{l,0}\frac{dv_0(t)}{dt} \\ &\quad -G_{nl,0}(v_0(t))v_0(t) - C_{nl}(v_0(t))\frac{dv_0(t)}{dt} \end{aligned} \tag{29a}$$

$$\begin{aligned} i_L(t) &= v_{sL}(t) - G_{l,L}v_L(t) - C_{l,L}\frac{dv_L(t)}{dt} \\ &\quad -G_{nl,L}(v_L(t))v_L(t) - C_{nl}(v_L(t))\frac{dv_L(t)}{dt} \end{aligned} \tag{29b}$$

It is to be pointed out that non-linear terminations can be directly incorporated into the model since the CRLH-LN is described in time-domain by (28). The overall equivalent circuit can be incorporated and simulated into a Spice-like non-linear solver [37].

5. NUMERICAL RESULTS

5.1. Comparison between the CRLH-LN and the Homogeneous CRLH-TL

In the first test the CRLH-LN described in Ref. [9] has been considered and the different dispersive behavior with respect to the homogeneous transmission line is investigated. The CRLH-LN is characterized by global parameters $R = 0.1\ \text{m}\Omega, L_R = 2.45$ nH, $C_L = 0.68$ pF, $G = 10$ mS, $C_R = 0.5$ pF and $L_L = 3.38$ nH and is constituted by 50 unit cells of length $\ell = 6.1$ mm.

Figure 6 shows the dispersion diagram β/ω of the CRLH-LN described in Ref. [9], using the Bloch-Floquet theorem [6], the approximated one under the hypothesis of electrically small sections and that of a homogeneous CRLH-TL. It is seen that the hypothesis of electrically small network and homogeneous transmission line leads to significantly different results from the Bloch-Floquet theorem in the gigahertz range.

In Ref. [9], it is shown that CRLH-LN is equivalent to the homogenous CRLH-TL for small electrical lengths and the dispersion relation obtained applying periodic boundary conditions reduces to the homogenous dispersion relation. Due to the left-handed lumped

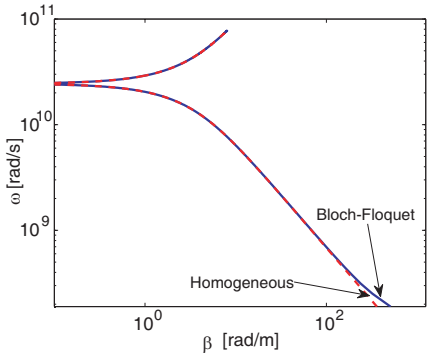

Figure 6. Dispersion diagram. The solid line refers to the Bloch-Floquet theorem, the dashed line refers to the homogeneous CRLN-TL (example 5.1).

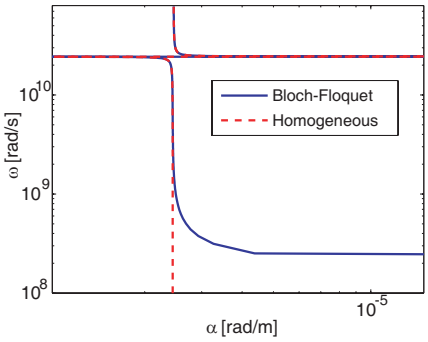

Figure 7. Attenuation constant (example 5.1).

elements C_L and L_L, for a fixed length ℓ of the unit-cell, the hypothesis of small electrical length fails to apply at low as well as high frequency, preventing the homogeneous transmission line model to be used for accurate broadband time-domain analysis of CRLH-LN structures. Figure 7 shows the attenuation constant α as evaluated using the homogeneous CRHL-TL and the CRLH-LN models. Again, a significant difference is observed up to few gigahertz. In particular, the CRLH-LN exhibits a frequency independent attenuation constant α at low frequencies while the homogeneous CRHL-TL is characterized by an almost constant value for decreasing frequencies.

The CRLH-LN is excited by the second derivative of a gaussian pulse whose magnitude frequency spectrum is shown in Figure 8.

The CRLH-LN is terminated on $50\,\Omega$ resistances. The macromodel of order 198 has been generated and simulated. Figure 9 shows the voltage at the input port computed using the inverse fast Fourier transform of the frequency-domain results obtained from the transmission line theory (CRLH-TL-IFFT) and the CRLH-LN (CRLH-LN-IFFT) and the proposed macromodeling technique (CRLH-LN-Macromodel). No significant difference is noticeable between the models of the CRLH-LN while a significant discrepancy is observed with respect to the homogeneous transmission CRHL-TL.

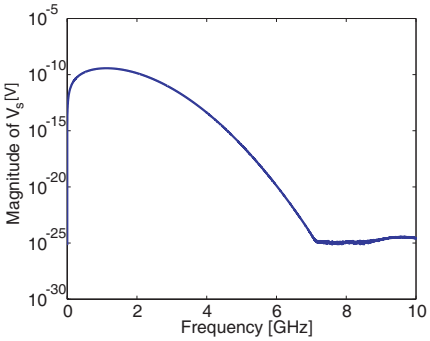

Figure 8. Magnitude spectrum of the voltage source driving the CRLH-LN (example 5.1).

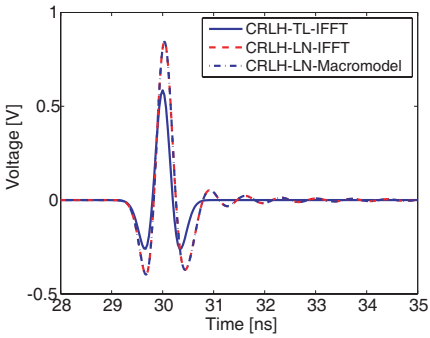

Figure 9. Input port voltage (example 5.1).

5.2. Time-domain Analysis of Unbalanced CRLH-LN

As a second example, it has been considered a lossy CRLH-LN composed of $n = 16$ unit cells of length $\ell = 1.5\,\text{cm}$ with the topology in Figure 5, with the circuital parameters $C_R = 4.5\,\text{pF}$, $C_L = 2.5\,\text{pF}$, $L_R = 4.5\,\text{nH}$ and $L_L = 2.5\,\text{nH}$, $R = 10\,\text{n}\Omega$, $G = 10\,\text{nS}$, corresponding to a transition frequency of about $f_0 = 1.5\,\text{GHz}$. The ladder network is excited by a gaussian pulse with amplitude 1 V and width 0.5 ns. Figure 10 shows the magnitude spectra of the $ABCD$ parameters of the global periodic structure as evaluated using the standard cascade of identical unit cells and the proposed closed-form polynomial approach, exhibiting a perfect overlapping.

It is clearly seen that there is substantial propagation in the 0.75–3 GHz range while frequencies below 0.75 GHz and above 3 are filtered. The rational model of order 16 has been generated and the Y parameters computed. Figure 11 shows the poles in the complex plane. It is easily recognized that the rational macromodel is stable since all the poles have negative real part. It is also easy to distinguish the poles corresponding to the zeros of the series impedance $Z_1(s)$, close to the imaginary axis, from the others derived from the $v_{j,n-1}$ roots, whose imaginary part is increasing with the order.

Figure 12 plots the magnitude spectra of the $Y_{11}(s)$ and $Y_{12}(s)$ functions of the global CRLH-LN structure as computed by direct transformation of the $ABCD$ parameters (CRLH-LN) and using the proposed polynomial model (CRLH-LN-pol). As before, the agreement is perfect. Again, the resonant behavior is clearly seen in the 0.75–3 GHz range.

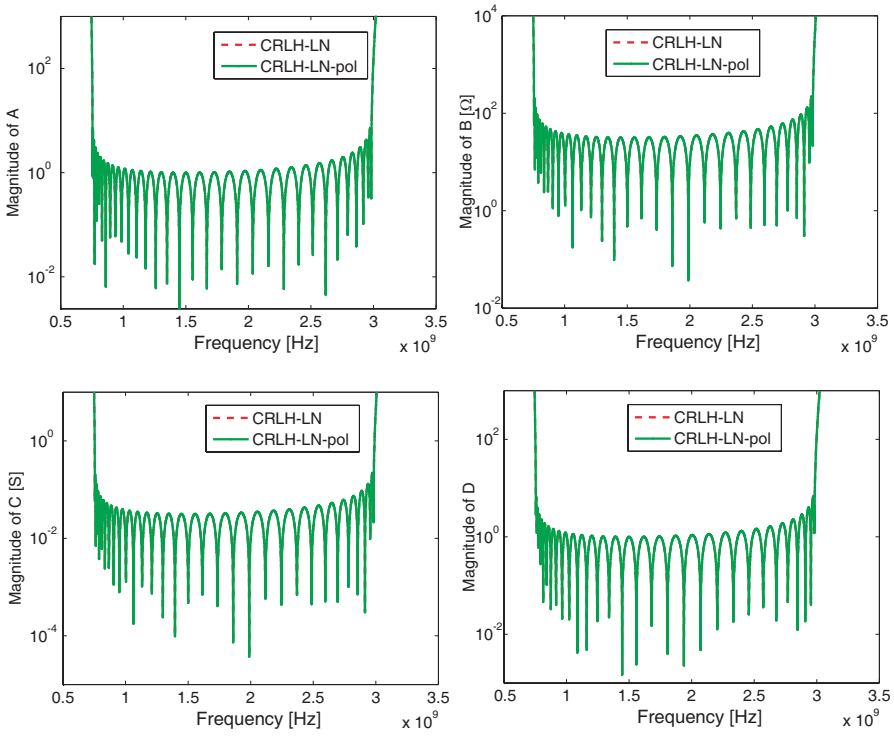

Figure 10. Magnitude spectra of the $ABCD$ parameters for the CRLH-TL (example 5.2).

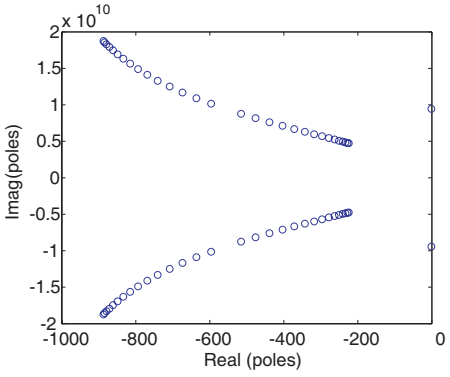

Figure 11. Poles of the CRLH-LN (example 5.2).

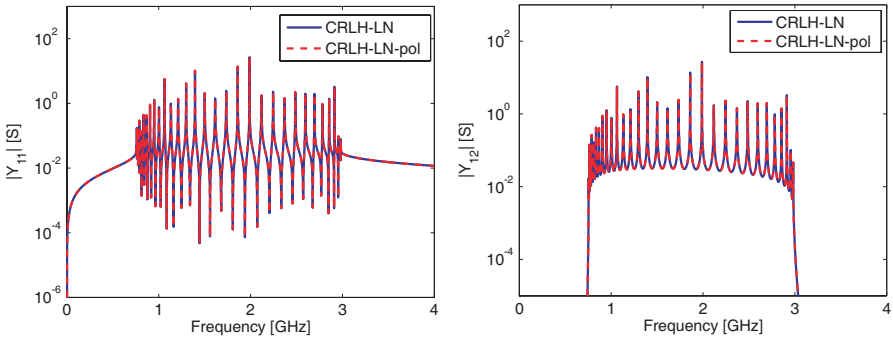

Figure 12. Magnitude spectra of Y_{11} and Y_{12} parameters (example 5.2).

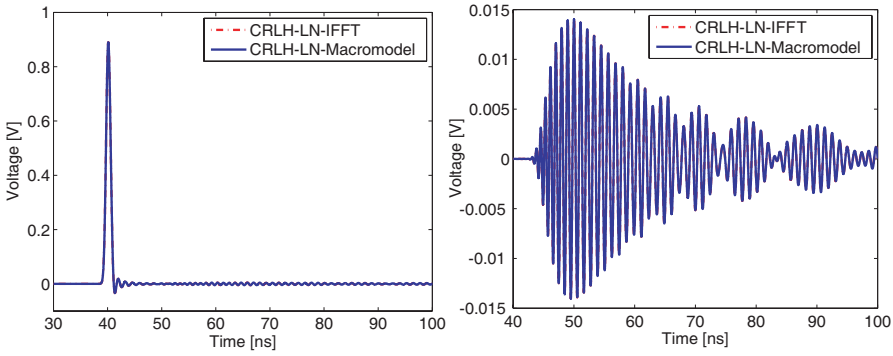

Figure 13. Port voltages of the CRLH-LN (example 5.2). Left: input port; right: output port.

The CRLH-LN is terminated on 50 Ω resistances. The time-domain macromodel is integrated using the Gear-Shichman algorithm [38]; the results are compared with those obtained by means of the inverse fast Fourier transform of the frequency data. Figure 13 shows the port voltages. The curves obtained by means of the two approaches are almost undistinguishable.

The time-domain results are compared by using the FSV technique. Figure 14 reports the FSV Grade-Spread chart for the input voltage of the first dipole as indicated by the IEEE Standard for data comparison [22]: the presence of the FSV figures of merits in the blue area indicates a high quality of the comparison for the data.

Then, in a second test, the output port of the CRLH-LN has been terminated in a non-linear lumped element defined by the following

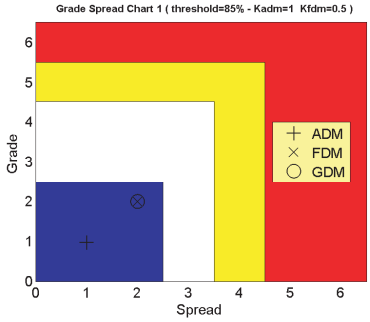

Figure 14. FSV comparison (example 5.2).

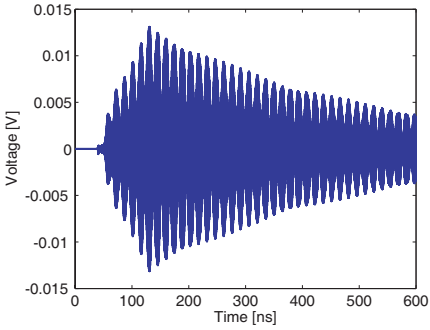

Figure 15. Output port voltage of the CRLH-LN terminated on a non-linear load (example 5.2).

equation $i(t) = 10v^3(t)$. The same macromodel has been used to compute the port voltages. The output port voltage is shown in Figure 15 where the dispersion due to the CRLH-LN is clearly visible.

6. CONCLUSIONS

In this paper, a general methodology for the analysis of CRLH-LNs has been presented. In particular the proposed method allows a rigorous rational model of the CRLH-LN. The rational model of the Y matrix permits an efficient identification of the poles/residues of the CRLH-LN, leading to a time-domain state-space model. The proposed methodology offers the following features:

- it can be applied to any type of CRLH-LN being independent on the topology of the unit cell [14, 18];
- if the unit cell admits a rational two port representation, the overall CRLH-LN is characterized by a rational model which is well suited for time-domain analysis; this means that dispersive behavior of lumped elements can be directly incorporated into the time-domain macromodel;
- since it does not use the inverse Fourier transform, it can directly handle non-linear terminations and can be linked to non-linear Spice-like solvers;
- it can be easily applied to coupled CRLH-LNs.

REFERENCES

1. Veselago, V. G., "The electrodynamics of substances with simultaneously negative values of ε and μ," *Usp. Fiz. Nauk.*, Vol. 92, 517–526, 1967 (in Russian).
2. Veselago, V. G., "The electrodynamics of substances with simultaneously negative values of ε and μ," *Sov. Phys. Usp.*, Vol. 47, 509–514, January–February 1968.
3. Smith, D. R., D. C. Vier, W. J. Padilla,, S. C. Nemat-Nasser, and S. Schultz, "Loop-wire for investigating plasmons at microwave frequencies," *Appl. Phys. Lett.*, Vol. 75, No. 10, 1425–1427, September 1999.
4. Smith, D. R., W. J. Padilla, D. C. Vier, S. C. Nemat-Nasser, and S. Schultz, "Composite medium with simultaneously negative permittivity and permeability," *Phys. Rev. Lett.*, Vol. 84, 4184–4187, May 2000.
5. Engheta, N. and R. W. Ziolkowski, "A positive future for double-negative metamaterials," *IEEE Transactions on Microwave Theory and Techniques*, Vol. 53, No. 4, 1536–1556, April 2005.
6. Caloz, C. and T. Itoh, *Electromagnetic Metamaterials: Transmission Line Theory and Microwave Applications*, Wiley-IEEE Press, 2005.
7. Eleftheriades, G. V. and K. G. Balmain, *Negative Refraction Metamaterials: Fundamental Principles and Applications*, Wiley-IEEE Press, 2005.
8. Caloz, C. and T. Itoh, "Transmission line approach of left-handed (LH) materials and microstrip implementation of an artificial LH transmission line," *IEEE Transactions on Antennas and Propagation*, Vol. 52, No. 5, 1159–1166, May 2004.
9. Lai, A., C. Caloz, and T. Itoh, "Composite right/left-handed transmission line metamaterals," *IEEE Microwave Magazine*, 34–50, September 2004.
10. Eleftheriades, G. V., O. Siddiqui, and A. K. Iyer, "Transmission line models for negative refractive index media and associated implementations without excess resonators," *IEEE Microwave and Wireless Components Letters*, Vol. 13, No. 2, 51–53, February 2003.
11. Grbic, A. and G. V. Eleftheriades, "Negative refraction, growing evanescent waves and sub-diffraction imaging in loaded transmission-line metamaterials," *IEEE Transactions on Antennas and Propagation*, Vol. 51, No. 12, 2297–2305, December 2003.
12. Sanada, A., C. Caloz, and T. Itoh, "Characteristics of the

composite right/left-handed transmission lines," *IEEE Microwave and Wireless Components Letters*, Vol. 14, No. 2, 68–70, November 2004.

13. Horii, Y., C. Caloz, and T. Itoh, "Super-compact multilayered left-handed transmission line and diplexer application," *IEEE Transactions on Microwave Theory and Techniques*, Vol. 53, No. 4, 1527–1534, April 2005.
14. Caloz, C., "Dual composite right/left-handed (D-CRLH) transmission line metamaterial," *IEEE Microwave and Wireless Components Letters*, Vol. 16, No. 11, 585–587, November 2006.
15. Rennings, A., S. Otto, J. Mosig, C. Caloz, and I. Wolff, "Extended composite right/left handed (E-CRLH) metamaterial and its application as quadband quarter-wavelength transmisson line," *Asia-Pacific Microwave Conference Digest*, Yokohama, December 2006.
16. Eleftheriades, G. V., "A generalized negative-refractive-index transmission line (NRI-TL) metamaterial for dual-band and quad-band applications," *IEEE Microwave and Wireless Components Letters*, Vol. 17, No. 6, 415–417, June 2007.
17. Rennings, A., T. Liebig, C. Caloz, and I. Wolff, "Double-Lorentz transmission line metameterials and its applications to tri-band devices," *IEEE Microw. Symposium Digest*, 1427–1430, Hololulu, Hawaii, USA, June 2009.
18. Camacho-Penalosa, C. and T. M. Martin-Guerrero, "Derivation and general properties of artificial lossless balanced composite right/left handed transmission lines of arbitrary order," *Progress In Electromagnetic Research B*, Vol. 13, 151–169, 2009.
19. Perruisseau-Carrier, J., R. Fritschi, P. Crespo-Valero, and A. K. Skrivervik, "Modeling of periodic distributed MEMS-application to the design of variable true-time delay lines," *IEEE Transactions on Microwave Theory and Techniques*, Vol. 54, No. 1, 383–392, January 2010.
20. Zhang, Y. and B. E. Spielman, "A stability analysis for timedomain method of moments analysis of 1-D double-negative transmission lines," *IEEE Transactions on Microwave Theory and Techniques*, Vol. 55, No. 9, 1887–1898, September 2007.
21. Gomez-Diaz, J. S., S. Gupta, A. Alvarez-Melcon, and C. Caloz, "Investigation on the phenomenology of impulse-regime metamaterial transmission lines," *IEEE Transactions on Antennas and Propagation*, Vol. 57, No. 12, 4010–4014, December 2009.
22. IEEE, Standard for Validation of Computational Electromagnetic (CEM) Computer Modeling and Simulation, and Recommended

Practice, Part I, IEEE, June 2008.

23. Duffy, A., A. Martin, A. Orlandi, G. Antonini, T. M. Benson, and M. Woolfson, "Feature Selective Validation (FSV) for validation of Computational Electromagnetics (CEM). Part I — The FSV Method," *IEEE Transactions on Electromagnetic Compatibility*, Vol. 48, No. 2, 449–459, August 2006.
24. Duffy, A., A. Martin, A. Orlandi, G. Antonini, T. M. Benson, and M. Woolfson, "Feature selective validation (FSV) for validation of computational electromagnetics (CEM). Part II — Numerical verification," *IEEE Transactions on Electromagnetic Compatibility*, Vol. 48, No. 2, 460–469, August 2006.
25. Frickey, D. A., "Conversion between S, Z, Y, h, $ABCD$ and T parameters which are valid for complex source and load impedances," *IEEE Transactions on Microwave Theory and Techniques*, Vol. 42, No. 2, 205–211, February 1994.
26. Pozar, D., *Microwave Engineering*, John Wiley and Sons, New York, 1998.
27. Ho, C., A. Ruehli, and P. Brennan, "The modified nodal approach to network analysis," *IEEE Transactions on Circuits and Systems*, Vol. 22, No. 6, 504–509, June 1975.
28. Pillegi, L., R. Rohrer, and C. Visweswariah, *Electronic Circuits and System Simulation Methods*, McGraw-Hill Book Company, 1995.
29. Faccio, M., G. Ferri, and A. D'Amico, "A new fast method for ladder networks characterization," *IEEE Transactions on Circuits and Systems*, I, Vol. 38, No. 11, 1377–1382, November 1991.
30. Antonini, G. and G. Ferri, "A new approach for closed-form transient analysis of multiconductor transmission lines," *IEEE Transactions on Electromagnetic Compatibility*, Vol. 46, No. 4, 529–543, November 2004.
31. Faccio, M., G. Ferri, and A. D'Amico, "The DFF and DFFz triangles and their mathematical properties," *Applications of Fibonacci Numbers*, G. E. Bergum et al., eds., Vol. 5, 199–206, 1990.
32. Antonini, G., "A new methodology for the transient analysis of lossy and dispersive multiconductor transmission lines," *IEEE Transactions on Microwave Theory and Techniques*, Vol. 52, No. 9, 2227–2239, September 2004.
33. Kailath, T., *Linear Systems*, Prentice Hall, Englewood Cliffs, NJ, 1980.
34. Chen, C. T., *Linear System Theory and Design*, Holt, Rinehart,

View publication stats

Winston, New York, 1984.

35. Ruberti, A. and S. Monaco, *Teoria dei Sistemi*, Pitagora Editrice Bologna, 1998.
36. Neumayer, R., A. Steltzer, F. Haslinger, and R. Weigel, "On the synthesis of equivalent-circuit models for multiports characterized by frequency-dependent parameters," *IEEE Transactions on Microwave Theory and Techniques*, Vol. 50, No. 12, 2789–2796, December 2002.
37. Nagel, L. W., "SPICE: A computer program to simulate semiconductor circuits," *Electr. Res. Lab. Report ERL M520*, University of California, Berkeley, May 1975.
38. Shichman, H., "Integration system of a nonlinear network analysis program," *IEEE Transactions on Circuits and Systems*, Vol. 17, 378–386, August 1970.